arXiv:0709.1566v1 [cond-mat.mes-hall] 11 Sep 2007

Spin polarized current in a junction of zigzag carbon nanotube

Zhan-Feng Jiang,[1,2] Jian Li,[2] Shun-Qing Shen,[2] and W. M. Liu[1]

[1]*Beijing National Laboratory for Condensed Matter Physics, Institute of Physics, Chinese Academy of Sciences, Beijing 100080, China*

[2]*Department of Physics, and Center of Theoretical and Computational Physics, The University of Hong Kong, Hong Kong*

(Dated: February 1, 2008)

We investigated spin-resolved electronic transport through a junction composed of a nonmagnetic metal electrode and a zigzag carbon nanotube (ZCNT) by means of self-consistent Green's function method in the tight binding approximation and the unrestricted Hartree-Fock approximation. Our results show that the electric current can be spin-polarized if the coupling of the junction is weak. Further calculations on spin-spin correlation and local density of states reveal the existence of magnetic edge states in ZCNTs, which is responsible for the observed spin-polarized current and can be controlled by applying a gate voltage. We also studied the influence of the nearest-neighbor Coulomb interaction and the junction coupling strength on the spin-polarization of the current.

PACS numbers: 73.22.-f, 73.63.Fg, 71.10.Hf, 77.22.Ej

I. INTRODUCTION

Carbon nanotubes (CNTs) have been the subject of a great amount of theoretical and experimental works during the past two decades, because of their rich and fascinating properties and potential applications in nanotechnology. Electronic structures and transport properties of infinite-length CNTs have been extensively studied and well understood.[1,2] A finite-length CNT, on the other hand, is usually treated only as a simplified one-dimensional quantum wire in transport theories,[3] or tunneling experiments,[4,5,6,7,8,9] with its crystal fine structures largely ignored. In fact, the hexagonal lattice structure of a CNT, inherited from the graphene lattice, may give rise to peculiar properties near its edges. One example is a recent work by Son *et al.*, where a zigzag graphene nanoribbon is predicted to be half-metallic when an strong-enough external electric field is applied transversely, due to its spin-polarized edge states.[10] Similarly the ground state of a ZCNT also shows antiferromagnetic order as a result of the Coulomb interaction and correlation of electrons in the hexagonal crystal lattice. This is explained by two mathematical theorems for the Hubbard model defined on a bipartite lattice with equal numbers of sublattice sites, *i.e.*, the ground state is a spin singlet[11] and the antiferromagnetic correlation is always dominant over other correlations.[12] Some literatures have investigated the band structures and antiferromagnetic orders (or spin density waves) in graphene ribbons or CNTs by the extended Hubbard Model.[13,14,15,16,17,18,19,20,21] Few works have been done, however, on the edge states of CNTs and their effects on transport.

In fact, not only zigzag graphene nanoribbons but also finite-length ZCNTs have spin-polarized edge states due to the Coulomb interaction and their bipartite lattice structures.[22] The spin polarized edge states existing in finite or semi-infinite ZCNTs can play an important role in their spin transport properties. Particularly, in a junction composed of a semi-infinite nonmagnetic metal (NM) electrode and a semi-infinite ZCNT, an edge state may exist in the ZCNT near the interface. The edge state is spin polarized, with oscillations upon different sublattices, and forms a spin-dependent scattering potential. It will act as a spin filter when electrons tunnel through the interface to induce a spin-polarized current. In this paper, we use the extended Hubbard model to investigate the spin-dependent transport of the junction of the ZCNT to the NM lead.

The paper is arranged as follows. In Sec.II we introduce the model Hamiltonian and describe the general formalism of our self-consistent method. In Sec.III, the main results and discussions are presented. Sec.IV is a brief summary, and finally, an appendix is attached to discuss the validity of the self-consistent method we used in this paper.

II. GENERAL FORMALISM

A. Model Hamiltonian

We consider a conjunction of a semi-infinite tubal lead and a semi-infinite ZCNT, each of which extends to an electron reservoir at infinity, as shown in Fig. 1(a). The ZCNT part is the standard hexagonal-crystal tube, and the NM part is assumed to be a square-lattice tube, which is connected to the terminal layer (layer-1 in Fig. 1(a)) of the ZCNT. In the tight-binding approximation, the model Hamiltonian for the whole system reads

$$H = H^L_{NM} + H^L_{int} + H_{NT}, \tag{1}$$

where

$$H_{NM}^{L} = -\sum_{\langle i,j\rangle,\sigma} t_L d_{i\sigma}^{+} d_{j\sigma} + \sum_{i,\sigma} V_L d_{i\sigma}^{+} d_{i\sigma}, \quad (2a)$$

$$H_{int}^{L} = -\sum_{\langle i,j\rangle,\sigma} t_{int}^{L} d_{i\sigma}^{+} c_{j\sigma} + h.c., \quad (2b)$$

$$H_{NT} = -\sum_{\langle i,j\rangle,\sigma} t c_{i\sigma}^{+} c_{j\sigma} + U\sum_{i} n_{i\uparrow} n_{i\downarrow} + V\sum_{\langle i,j\rangle} n_i n_j + V_{NT}\sum_{i,\sigma} n_{i\sigma}. \quad (2c)$$

Here, H_{NM}^{L} describes the semi-infinite NM lead, and $d_{i\sigma}^{+}(d_{i\sigma})$ is the creation (annihilation) operator of an electron at the ith site in the NM part with spin-σ ($\sigma =\uparrow,\downarrow$). $\langle i,j\rangle$ denotes a pair of nearest-neighboring sites i and j in the lattice, and t_L represents the hopping integral between them, and V_L is the electrostatic potential in the NM part. H_{int}^{L} represents the tunneling process between the NM lead and the ZCNT. In Fig. 1(a), $t_{int}^{L} \neq 0$ connects the interface layers of the NM lead and the ZCNT. H_{NT} describes the π-orbital electrons of the zigzag nanotube. We adopt the extended Hubbard model including the on-site Coulomb interaction U and nearest-neighbor interaction V.[16,17,23] $c_{i\sigma}^{+}(c_{i\sigma})$ is the creation (annihilation) operator of an electron at the ith site in the ZCNT with spin-σ, $n_{i\sigma} = c_{i\sigma}^{+} c_{i\sigma}$, and t is the hopping integral, which is about 2.7eV for carbon nanotubes,[24] taking the unit of energy in this paper. V_{NT} is the electrostatic potential in the ZCNT.

To solve the interacting problem, we perform the unrestricted Hartree-Fock approximation, and reduce H_{NT} to a mean-field one,

$$h_{NT} = -\sum_{\langle i,j\rangle,\sigma} (t + V\left\langle c_{j\sigma}^{+} c_{i\sigma}\right\rangle) c_{i\sigma}^{+} c_{j\sigma} + V_{NT}\sum_{i,\sigma} n_{i\sigma} + U\sum_{i}(\langle n_{i\uparrow}\rangle n_{i\downarrow} + \langle n_{i\downarrow}\rangle n_{i\uparrow}) + V\sum_{\langle i,j\rangle}\langle n_i\rangle n_j, \quad (3)$$

where the expectation values of physical quantities $\langle\cdots\rangle$ need to be calculated self-consistently. We use the zero-temperature Green's function method to establish a set of mean field equations, and calculate these expectation values for the system self-consistently. The technique of principal layers is used to solve the Green's function of a semi-infinite lead.[25,26] This technique, limited to treat periodic structures, is suitable for the NM lead, but not for the ZCNT part, because the inhomogeneity of $\left\langle c_{j\sigma}^{+} c_{i\sigma}\right\rangle$ and $\langle n_{i\sigma}\rangle$ near the interface of the ZCNT will make the mean-field Hamiltonian h_{NT} generally not a periodic one and thus we cannot apply this technique directly. But we notice that the expectation values deep inside the ZCNT part are nearly periodic and very close to the corresponding values in an infinite ZCNT. So we divide the ZCNT into two part: the central part with N units (see Fig. 1(a) for the definition of 'unit' in this paper) including the interface, and the semi-infinite right part. We assume the expectation values in the right part are periodic, in this way the Green's function of the right part can now be solved with the technique of principal layers and the whole system can be solved self-consistently. Thus although the whole system in Fig. 1 has only two compositions, in practice we treat it in three parts: the NM part on the left naturally, N units of the ZCNT including the interface at the center, and the rest of the ZCNT on the right. The assumption that the expectation values $\left\langle c_{j\sigma}^{+} c_{i\sigma}\right\rangle$ and $\langle n_{i\sigma}\rangle$ are periodic in the right part, and equal to those in an otherwise integral ZCNT, is justified when N is so large that the expectation value of any quantity in the ZCNT changes little with increased N. In Appendix we will discuss this issue in more details. Based on the above analysis, the Hamiltonian for the ZCNT can be rewritten as

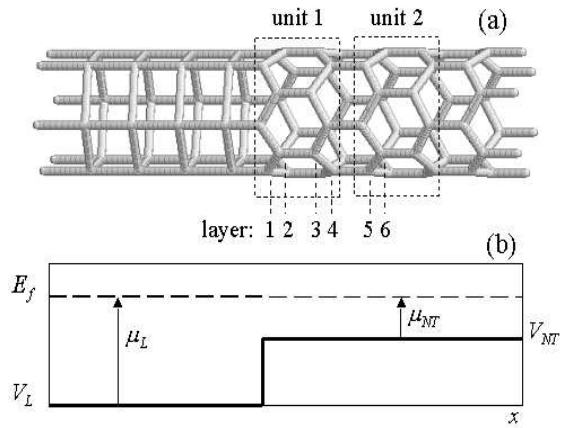

FIG. 1: (a) Schematic of a NM-ZCNT junction, the dashed rectangles denote the unit cells of ZCNT, and the dashed lines denote the layers of ZCNT. (b) Schematic diagram of the electrostatic potential and electrochemical potential.

$$h_{NT} = h_{NT}^{M} + h_{int}^{R} + h_{NT}^{R}, \quad (4)$$

where h_{NT}^{M} and h_{NT}^{R} describe the central part and the semi-infinite right part, respectively, $h_{int}^{R} = -\sum_{\langle i,j\rangle,\sigma}(t + V\left\langle c_{j\sigma}^{+} c_{i\sigma}\right\rangle) c_{i\sigma}^{+} c_{j\sigma}$ represents the connection between the central part h_{NT}^{M} and the right part h_{NT}^{R}. In this way, h_{NT}^{R} can be treated by the technique of principal layers.

In order to reduce the influence of band structure of the nonmagnetic metal lead on the transport property, we take $t_L = 4t$, which is equivalent to the so-called "wide-band limit".[27] And in order to preserve the edge state of the ZCNT, we take $t_{int}^{L} = 0.1t$, which is a comparatively small value implying weak coupling between the NM lead and the ZCNT, or a high potential barrier between them. This can be realized in experiments by fabricating an oxide layer at the interface.[3] In equilibrium, the Fermi level of the whole system E_f is identical everywhere as shown in Fig. 1(b). Following the definitions in Ref.

[28], the electrochemical potential (ECP) in the ZCNT is defined by $\mu_{NT} \equiv E_f - V_{NT}$, and the electrochemical potential in the NM part is defined by $\mu_L \equiv E_f - V_L$. In this paper, E_f, V_L, and μ_L are fixed, V_{NT} is assumed to be adjustable by means of a gate voltage. Adjusting μ_{NT} may control the electron density n_e in the ZCNT. We will fix the NM part at half-filling by tuning V_L (or μ_L), so that the transport modes in the left lead around the Fermi level can match those in the ZCNT, to facilitate the electronic transport.[29]

B. Method

We come to establish the mean field equation by means of the self-consistent Green's function method, and then to use the recursive method to find the numerical solution. The retarded Green's function is defined by

$$G^r_{i\sigma,j\sigma'}(t;t') = -i\theta(t-t')\left\langle\left\{c_{i\sigma}(t), c^+_{j\sigma}(t')\right\}\right\rangle, \quad (5)$$

whose Fourier transform can be calculated by the Dyson's Equation[30]

$$G^r(E) = \frac{1}{E + i\eta - h^M_{NT} - \Sigma_L(E) - \Sigma_R(E)}, \quad (6)$$

where η is an infinitesimal constant, and h^M_{NT} is the mean-field Hamiltonian of the central part as defined in the last subsection. $\Sigma_L = H^{L+}_{int} g^r_L H^L_{int}$ is the self-energy due to the left lead, where H^{L+}_{int} is the Hermitian conjugate of H^L_{int} and $g^r_L = (E + i\eta - H^L_{NM})^{-1}$ is the retarded Green's function of the left lead. The self-energy due to the right lead has the similar definition $\Sigma_R = h^{R+}_{int} g^r_R h^R_{int}$ and $g^r_R = (E + i\eta - h^R_{NT})^{-1}$. In the present approach, the system is defined on a lattice and the Hamiltonian h^M_{NT} as well as the self energy can be re-expressed in the form of square matrix. The dimensionality of the matrix is twice of the lattice number of the cental part of carbon nanotube because the spin degree of freedom. For a finite number of lattice sites, the Green's function can be calculated numerically once the initial values are assigned to the expected quantities in Eq.(3) such as the local densities of charge and spin. Once we have this Green's function, the expectation value of any physical quantity can be obtain as follows

$$\left\langle c^+_{i\sigma} c_{j\sigma'}\right\rangle = \frac{1}{2\pi i}\int_{-\infty}^{E_f} dE \cdot [G^{r*}_{i\sigma,j\sigma'}(E) - G^r_{j\sigma',i\sigma}(E)], \quad (7)$$

where $G^{r*}_{i\sigma,j\sigma'}(E)$ is the complex conjugate of $G^r_{i\sigma,j\sigma'}(E)$. Then the local charge and spin density are given by

$$n_e(i) = \left\langle c^+_{i\uparrow} c_{i\uparrow} + c^+_{i\downarrow} c_{i\downarrow}\right\rangle, \quad (8)$$

and

$$S(i) = \left\langle c^+_{i\uparrow} c_{i\uparrow} - c^+_{i\downarrow} c_{i\downarrow}\right\rangle, \quad (9)$$

respectively.

The recursive method is applied to obtain the stable solution for the problem. The stable solutions of the Green's functions are applied to calculate the relevant physical quantities. The spin polarization (SP) of the conductance is defined by

$$S_P \equiv \frac{G_\uparrow - G_\downarrow}{G_\uparrow + G_\downarrow}, \quad (10)$$

where G_σ is the conductance in the spin-σ channel ($\sigma = \uparrow, \downarrow$), which is given by the Landauer's formula,

$$G_\sigma = \frac{e^2}{h} Tr[\Gamma_{L\sigma} G^r \Gamma_{R\sigma} G^{r+}]_{E=E_f}, \quad (11)$$

where $\Gamma_{A\sigma} \equiv i(\Sigma_{A\sigma} - \Sigma^+_{A\sigma})$, and $\Sigma_{A\sigma}$ represents the self-energy of lead A ($= L, R$) in the spin-σ subspace, G^{r+} is the Hermitian conjugate of G^r.

For concreteness, we describe the overall procedure of the present self-consistent calculation, which is illustrated in a flow chart in Fig. 2 and elucidated as follows:

Step 1: Calculate the self-energy due to the left lead. Because there's no Coulomb interaction term in the Hamiltonian of the left lead, we can solve this part without recursion. An arbitrary value can be assigned to V_{NM} to complete the Hamiltonian H^L_{NM}, then $g^r_L(E)$ and $\Sigma_L(E)$ can be calculated by the technique of principal layer[25,26]. It's found that the left lead is half-filled when the Fermi energy $E_f = V_L$, as the left lead is a simple square lattice. The Fermi level E_f is identical for the whole system because we are studying in the linear response regime, and it is kept unchanged in the following steps.

Step 2: Construct a trial Hamiltonian h_{NT}. An initial charge and spin distribution is assigned in the zigzag nanotube. The initial change density promises that the number of electrons per site is about 1, which represents the half-filled case of the zigzag nanotube. Spin density wave and charge density wave are constructed on the zigzag nanotube at the same time, because many literatures have referred to the coexistence of the spin density wave and charge density wave in carbon nanotubes or ribbons[16,17,20,21], and this is also a general property of the half-filled extended Hubbard model[31,32]. The hopping term $\left\langle c^+_{j\sigma} c_{i\sigma}\right\rangle$ is assigned to be 0, because we have no knowledge about it so far. Remember $\left\langle c^+_{j\sigma} c_{i\sigma}\right\rangle$ and $\langle n_{i\sigma}\rangle$ in the right unit of the central part is also used to determine the Hamiltonian h^R_{int} and h^R_{NT}. The electrostatic potential V_{NT} can be assigned the same value with E_f at first, because all cases are nearly half-filled. V_{NT} will be changed in the following iterations. Although V_{NT} is fixed by the gate voltage in experiments, we cannot use it to be the restrictive condition in the calculation, otherwise the iterations won't converge. We use the local charge density n_e in the right lead to be the restrictive condition, which can lead to convergence. Because n_e has a one-to-one correspondance to V_{NT}, V_{NT} will be determined along with the procedure of convergence.

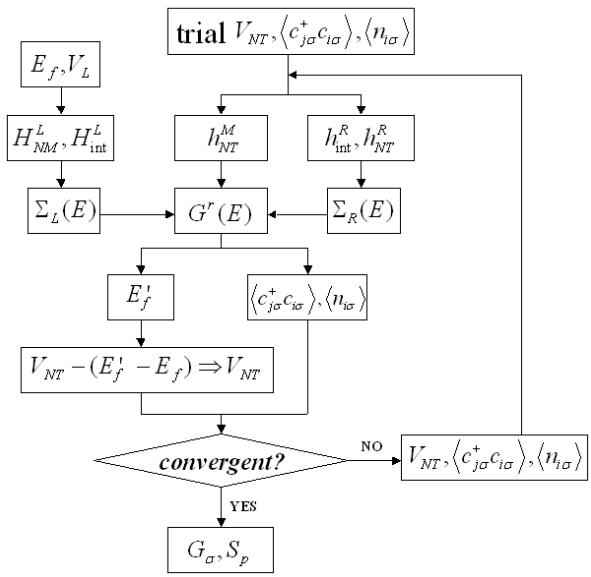

FIG. 2: The flow chart of the self-consistent calculation.

Step 3: Calculate the Green's function $G^r(E)$ in Eq.(6). The self-energy $\Sigma_R(E)$ can be obtained from the Hamiltonian h^R_{int} and h^R_{NT}.

Step 4: Calculate the expectation values of the physical quantities $\langle c^+_{j\sigma} c_{i\sigma} \rangle$ and $\langle n_{i\sigma} \rangle$ from Eq.(7) and (8), and find a new Fermi energy E'_f. The restrictive condition for finding E'_f is the local charge density n_e in the right lead is a certain value. After that we have to draw the Fermi energy back to the initial value E_f by means of tuning V_{NT}. So we substitute $V_{NT} - (E'_f - E_f)$ for V_{NT}.

Step 5: Judge the convergence. If the expectation values of the physical quantities $\langle c^+_{j\sigma} c_{i\sigma} \rangle$ and $\langle n_{i\sigma} \rangle$ has converged, we can end the iterations and get the stable solutions. Otherwise we have to use V_{NT}, $\langle c^+_{j\sigma} c_{i\sigma} \rangle$ and $\langle n_{i\sigma} \rangle$ to update the Hamiltonian h_{NT}, then turn to step 3 to begin a new iteration.

Step 6: After convergence, we use the the stable solutions of the Green's functions to calculate the spin polarization of conductance by Eq.(10) and (11).

When we calculate the expectation values from Eq.(7), for the sake of precision, we employ the contour integration in the complex energy plane[33], instead of direct integration along the real energy axis, because the retarded Green's function can be analytically continued into the complex energy plane. On the integration path, the complex energy has a large imaginary part, so the infinitesimal constant η in Eq.(6) becomes negligible, even can be assigned 0. But when we calculate Eq.(11), the constant η becomes indispensable. It should be assigned a value as small as possible, so that the conductances are not influenced by it.

On the magnitudes of U and V, U was adopted in a range of $2t \sim 4t$ and $V \approx t$ for graphene, ribbons or nanotubes in some literatures[14,17,23]. They were estimated from some organic molecules or by fitting the exciton energies of nanotubes. People also try to use the first principle calculations to obtain the values of U and V. But as the authors of the Ref. [20] pointed out, the values of these parameters depend on the choice of the exchange-correlation functional used within the calculation of density-functional theory. For example, U is chosen at $0.9t \sim 2t$ when one studied the problem of edge states[20]. Here we adopt this result to discuss the effect of U and V in several cases.

III. RESULTS AND DISCUSSION

A. The case of $V = 0$

In this section, we first consider the case of $V = 0$ and focus on the effect of U, since it is U, rather than V, that is one of the essential factors to stabilize the spin-polarized edge states. We choose $U = 1.2t$ in this subsection. And the ZCNT's configuration is (6,0), which is metallic when the Coulomb interaction is ignored.[1]

Fig. 3(a) shows the spin-resolved conductance as a function of the relative electrochemical potential of the ZCNT, defined by $\Delta\mu_{NT} = \mu_{NT} - \mu^0_{NT}$, where μ^0_{NT} is the electrochemical potential of the ZCNT in the half-filled case. And Fig. 3(b) shows the spin polarization of the conductance, calculated from the data in Fig. 3(a). We divide the electrochemical potential into three parts, according to the spin polarization. In region A and C, the spin polarization of the conductance is zero, while the spin polarization is not equal to zero and even may change its sign in region B. In order to understand this phenomenon, we investigate the energy levels of the edge of the ZCNT, *i.e.*, layer 1 in Fig. 1(a).

In Fig. 4, the square (diamond) markers denote the energy level of the edge state with spin-$\uparrow(\downarrow)$, which are obtained by locating the peaks of the spin-resolved local density of states (LDOS) in layer 1. The abscissa n_e is the electron density deep inside the ZCNT, by our previously stated assumption it takes the value of the electron density at the right side of the central ZCNT, or equally in the right ZCNT part. The zero point of energy is chosen to be at $\mu_{NT} = \mu^0_{NT}$. The straight line describes the dependence of the relative electrochemical potential $\Delta\mu_{NT}$ on the electron density n_e. The linear relation between them implies a constant density of states (DOS) and linear dispersion relations around the Fermi level of the ZCNT. We again divide the whole range into three parts according to the relative magnitudes of the energy levels of the edge states and the electrochemical potential of the ZCNT. We notice that this division is in accordance with Fig. 3, *i.e.*, the energy levels of the edge states overlap in region A and C, but split in region B.

In region A, $\Delta\mu_{NT}$ is below the energy levels of two edge states, which are both empty. The charge density n_e in layer 1 is very low as shown in Fig. 5(a), and the spin density $S(i)$ is zero everywhere as shown in Fig. 5(b).

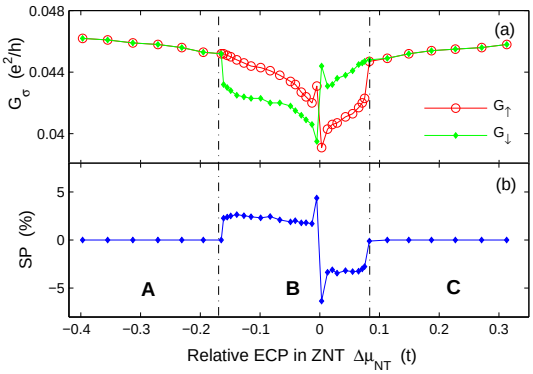

FIG. 3: (Color online) (a) Spin-resolved conductance and (b) Spin polarization of the conductance of the NM-ZCNT junction, as functions of the relative electrochemical potential of the ZCNT. The division of the region A, B and C is according to the magnitude of the SP.

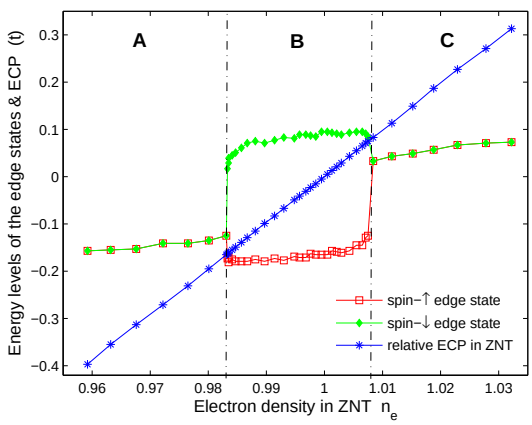

FIG. 4: (Color online) The energy levels of the edge states and the relative ECP in ZCNT as functions of electron density in the ZCNT. The whole range is divided into three regions according to the relative magnitudes of the energy levels of the edge states and the ECP of ZCNT, in accordance with Fig. 3.

Thus the charge current is not spin polarized through the junction in region A of Fig. 3. In region B, $\Delta\mu_{NT}$ is between the energy levels of two edge states, thus only one of them is occupied. This leads to a high spin density in layer 1 with its charge density nearly equal to that in other layers as shown in Fig. 5(a). The spin density oscillates in antiferromagnetic order in the next several units and decays rapidly as shown in Fig. 5(b), which is the same as expected in Refs.[11,12]. The spin-polarized edge state acts as a spin-dependent barrier, and makes the current through the junction spin-polarized in region B. In region C, $\Delta\mu_{NT}$ is above the energy levels of both edge states, which are occupied. The charge density in

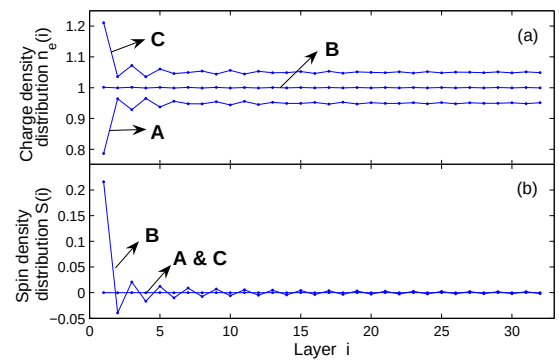

FIG. 5: (Color online) (a) Electron's charge and (b) spin density distribution along the ZCNT in the three configurations A, B and C.

layer 1 is very high as shown in Fig. 5(a), and the spin density is zero everywhere once again in Fig. 5(b). So there's no spin-polarized current through the junction.

Furthermore, Fig. 3(b) shows an approximate antisymmetry, but not an exact one. This fact reflects the partial particle-hole symmetry of the Hubbard model on a biparticle lattice.[11,12] As we can see in Fig. 1, either the NM part or the ZCNT part is of biparticle lattice, but the tunneling terms between them H^L_{int} break the bipartite structure of the whole system, and the symmetry is broken. However because of a weak H^L_{int}, the SP still exhibits the antisymmetry approximately.

This subsection contains the main result of this paper, it describes three phases of the edge of the ZCNT. They can emerge consequently by increasing the electron densities or the electrochemical potentials of the ZCNT. As a result the transition between these phases can be realized by adjusting the gate voltage applied on the ZCNT in experiments.

B. The case of $V \neq 0$

In this subsection, we investigate the effect of the nearest-neighbor Coulomb interaction V. We take $U = 2t$, and compare the spin polarization in the cases of $V = 0$, $0.05t$, $0.1t$, $0.2t$, and $0.4t$. Fig. 6 shows the SP of the conductance as a function of the electron density in the ZCNT, which indicates that V has two effects on the SP.

(i) When V increases, the region of non-zero S_p moves leftward. This means that the energy levels of the edge states become lower from the middle of the whole band as V increases, which can be understood from the band structure of the zigzag nanoribbons in Ref.[10] because the energy levels of the edge states of ZCNT can be obtained from the flat bands of the zigzag nanoribbons by means of the band-folding approach.[1] The flat bands in Fig. 2(c) of Ref.[10] are lowered from the middle of the

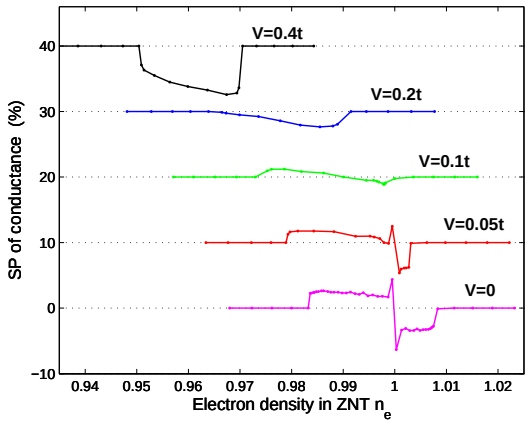

FIG. 6: (Color online) Spin polarization of conductance as a function of electron density in the ZCNT for different values of the nearest-neighbor Coulomb interaction strength V, with vertical offsets of 10% for clarity.

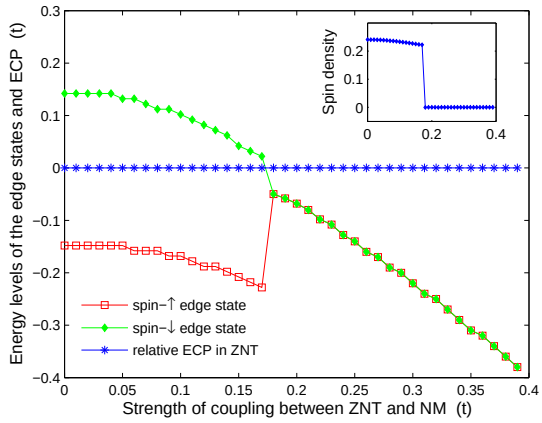

FIG. 7: (Color online) The energy levels of the edge states and the relative ECP in ZCNT as functions of the coupling strength between the ZCNT and NM electrode. The inset shows the spin density on the edge of the ZCNT as a function of the coupling strength. The parameters are $U = 1.2t$, $V = 0$.

whole band, and the same mechanism also happens in ZCNTs. Now we know it attributes to the effect of the nearest-neighbor Coulomb interaction V.

(ii) When $V = 0$, the spin polarization of the conductance is nearly antisymmetric. The position of the sign change is about at $n_e = 1$, *i.e.*, the half-filling point as shown in Fig. 3. This property is relevant to the partial particle-hole symmetry of the Hamiltonian Eq. (2c) at $V = 0$,[11,12] and the weak tunneling limit. But the antisymmetry is broken as V increases, the region of $S_P < 0$ expands leftward in Fig. 6. Thus we may conclude that in the cases with $V = 0.2t$, $0.4t$, as in Fig. 6, the lack of any sign change in the spin polarization of the conductance is a result of the nearest-neighbor Coulomb interaction V.

C. Effect of the coupling strength

In this subsection, we investigate the effect of the coupling between the ZCNT and the NM part. Fig. 7 illustrates the energy levels of the edge states and the relative ECP in the ZCNT as functions of the coupling strength between the ZCNT and NM electrode. The relative ECP is always zero because the ZCNT we study in this subsection is always half-filled. We can see the energy levels of the edge states shift down when the strength of coupling increases. There's a sudden change around $t^L_{int} = 0.17t$, where the two energy levels of the edge states are both occupied. This is a transition from the single to double occupancy on the edge of the ZCNT. Because the edge states are spin-polarized, the transition is also accompanied by a magnetic transition at the edge. The inset shows the spin density on the edge of the ZCNT as a function of the coupling strength t^L_{int}. When the edge states are single-occupied, the edge of the ZCNT is magnetic. However, the magnetism of the edge disappears suddenly at $t^L_{int} = 0.17t$ when the two edge states are both occupied, and the spin polarizations of the two states cancel each other.

IV. CONCLUSION

In summary, we have investigated the spin polarized transport in a junction of a nonmagnetic metal lead and a zigzag carbon nanotube. Due to Coulomb interaction of electrons, the zigzag carbon nanotube indicates strong antiferromagnetic correlation at half-filling, which is enhanced near the edge. The effect of the magnetic edge states leads to spin polarization of the electronic transport.

Compared with the half-metallic zigzag graphene nanoribbons in Ref. [10], the NM-ZCNT junction device we present here can be fabricated more easily because of the developed synthesis technique of carbon nanotubes, though the spin polarization is weaker than that of the zigzag nanoribbons, which can be 100% because of their half-metallic property. In both cases edge states are the keys in generating spin polarization, but they act in different ways. The edge states of a nanoribbon carry spin-polarized currents, while the edge state in our nonmagnetic metal-zigzag carbon nanotube junction does not, actually it blocks the current in a spin-dependent manner to produce spin polarization. The spin filter function of a ZCNT hasn't been discovered in experiments so far. This is possibly because the contact between the nanotube and the electrode has allowed the current to enter the nanotube without crossing the edge, as shown in Fig. 1 of Ref. [34]. This type of contact is called "side-contact" in Ref. [35]. What we need is the so-called "end-contact",

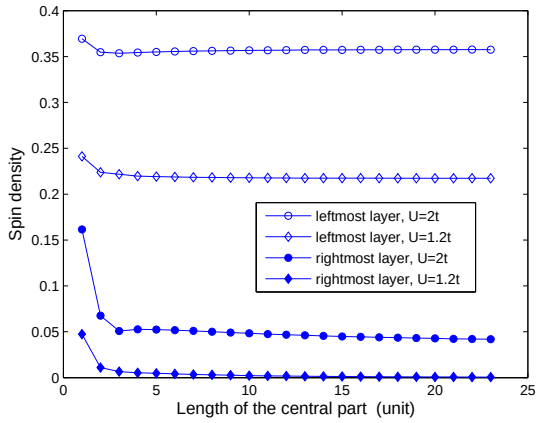

FIG. 8: (Color online) Spin densities in the leftmost and rightmost layer of the central part as functions of the lengh of the central part for $U = 1.2t$ and $2t$, $V = 0$. The spin density in the rightmost layer is multiplied by (-1).

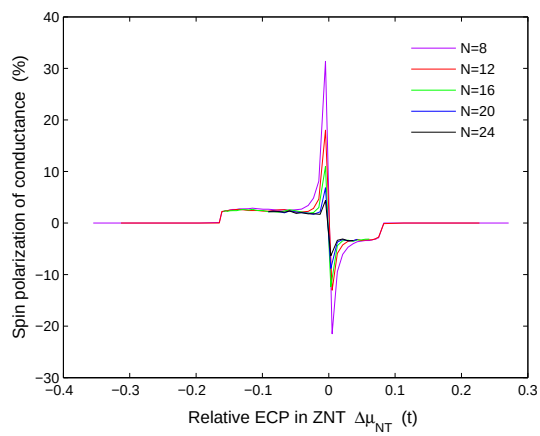

FIG. 9: (Color online) Spin polarization of conductance as a function of the relative electrochemical potential of ZCNT for different length of the central part N=8,12,16,20,24.

and the coupling between the ZCNT and the NM electrode must be weak enough to preserve the edge state of the ZCNT. This way the junction may act as a spin filter and produce spin-polarized tunneling current.

Acknowledgments

We thank Guan-Hua Chen and Fan Wang for useful discussions. This work was supported by NSF of China under grant 90406017, 60525417, the NKBRSF of China under Grant 2006CB921400, and the Research Grant Council of Hong Kong under grant No.: HKU 7042/06 (S.Q.S).

Appendix: Validity of the self-consistent method

In the Sec. II(A), in order to use the technique of the principal layer[25,26] to calculate the Green's function of the semi-infinite ZCNT lead, we divide the NM-ZCNT junction into three part: the left NM lead, the central ZCNT part, and the right ZCNT lead. We take the left N units of the ZCNT as the central part, and the rest of the ZCNT as the right semi-infinite lead. It is assumed that the right ZCNT lead has the mean-field Hamiltonian h^R_{NT} with periodic distribution of local charge and spin densities. This assumption becomes reasonable only when the length of the central part N is large enough such that the edge effect vanishes completely to the bulk properties. For a large N, the expectation of any physical quantity in the ZCNT lead is assumed to be independent of N. We investigate the spin densities in the leftmost and rightmost layers of the central part as functions of N in Fig. 8. It can be seen that the expectation values converge quickly as N gets larger. The spin density in the leftmost layer is large to form a magnetic edge state. The spin density in the rightmost layer, which is multiplied by -1 in Fig. 8, is small, and converges to the amplitude of the spin density wave in an infinite ZCNT[16]. By the way, we have used the self-consistent Green's function method on the infinite nanotubes, and recovered the results in Ref. [16].

Further more, we compare the SP of conductance for different length of the central part, as shown in Fig. 9. As N increases, most of the SP do not change except the region of sign reversal. The peaks of SP become lower as N increases. Due to the restriction of our computer's ability, we just take $N = 24$ for the central part in this paper, and keep in mind the SP of conductance we calculated may not be very accurate around the point of sign reversal.

We also make an error estimation of the self-consistent method. We run 10 more iterations after the condition of convergence has been satisfied, and calculate the relative standard deviation of S_p. The relative standard deviation are all less than 1% for dozens of random samples.

[1] J. C. Charlier, X. Blase, and S. Roche, Rev. Mod. Phys. **79**, 677 (2007).

[2] R. Saito, G. Dresselhaus, and M. S. Dresselhaus, *Physical*

Properties of Carbon Nanotubes, ICP Press (World Scientific, Singapore, 1998)
[3] A. Cottet, T. Kontos, S. Sahoo, H. T. Man, M. S. Choi, W. Belzig, C. Bruder, A. Morpurgo, and C. Schoenenberger, Semicond. Sci. Technol. **21**, S78 (2006).
[4] W. Liang, M. Bockrath, D. Bozovic, J. H. Hafner, M. Tinkham, and H. Park, Nature (London) **411,** 665 (2001).
[5] S. J. Tans, M. H. Devoret, R. J. A. Groeneveld, and C. Dekker, Nature (London) **394**, 761 (1998).
[6] S. Sahoo, T. Kontos, , J. Furer, C. Hoffmann, M. Gräber, A. Cottet, and C. Schönenberger, Nature Phys. **1**, 99 (2005).
[7] H. T. Man, I. J. W. Wever, and A. F. Morpurgo, Phys. Rev. B **73**, 241401(R) (2006).
[8] A. Jensen, J. R. Hauptmann, J. Nygård, and P. E. Lindelof, Phys. Rev. B **72**, 035419 (2005).
[9] L. E. Hueso, J. M. Pruneda, V. Ferrari, G. Burnell, J. P. Valdés-Herrera, B. D. Simons, P. B. Littlewood, E. Artacho, A. Fert, and N. D. Mathur, Nature (London) **445**, 410 (2007).
[10] Y. W. Son, M. L. Cohen, and S. G. Louie, Nature (London) **444**, 347 (2006).
[11] E. H. Lieb, Phys. Rev. Lett. **62**, 1201 (1989).
[12] S. Q. Shen, Z. M. Qiu and G. S. Tian, Phys. Rev. Lett. **72**, 1280 (1994); S. Q. Shen, Inter. J. Mod. Phys. B **12,** 709 (1998).
[13] M. Fujita, K. Wakabayashi, K. Nakada, and K. Kusakabe, J. Phys. Soc. Jpn. **65**, 1920 (1996).
[14] A. L. Tchougreeff and R. Hoffmann, J. Phys. Chem. **96**, 8993 (1992).
[15] K. Kobayashi, J. Chem. Phys. **106**, 8746 (1997).
[16] M. P. López Sancho, M. C. Muñoz, and L. Chico, Phys. Rev. B **63**, 165419 (2001).
[17] A. Yamashiro, Y. Shimoi, K. Harigaya, and K. Wakabayashi, Phys. Rev. B **68**, 193410 (2003).
[18] A. Yamashiro, Y. Shimoi, K. Harigaya, and K. Wakabayashi, Physica E **22**, 688 (2004).
[19] K. Harigaya, A. Yamashiro, Y. Shimoi, K. Wakabayashi, Curr. Appl. Phys. **4**, 587 (2004).
[20] L. Pisani, J. A. Chan, B. Montanari, and N. M. Harrison, Phys. Rev. B **75**, 064418 (2007).
[21] F. Ye, B. S. Wang, J. Z. Lou, and Z. B. Su, Phys. Rev. B **72**, 233409 (2005).
[22] H. H. Lin, T. Hikihara, B. L. Huang, C. Y. Mou, X. Hu, arXiv: cond-mat/0410654v2
[23] Z. D. Wang, H. B. Zhao, and S. Mazumdar, Phys. Rev. B **74**, 195406 (2006).
[24] Y. W. Son, M. L. Cohen, and S. G. Louie, Phys. Rev. Lett. **97**, 216803 (2006).
[25] J. Zhang, Q. W. Shi, and J. Yang, J. Chem. Phys. **120,** 7733 (2004);
[26] D. H. Lee and J. D. Joannopoulos, Phys. Rev. B **23**, 4988 (1981); **23**, 4997 (1981).
[27] A. P. Jauho, N. S. Wingreen, and Y. Meir, Phys Rev B **50**, 5528 (1994).
[28] A. Rycerz, J. Tworzyło, and C. W. J. Beenakker, Nature Phys. **3**, 172 (2007).
[29] D. K. Ferry and S. M. Goodnick, *Transport in Nanostructures* (Cambridge University Press, New York, 1995).
[30] S. Datta, *Electronic transport in mesoscopic system* (Cambridge University Press, New York, 1997).
[31] J. E. Hirsch, Phys. Rev. Lett. **53**, 2327 (1984).
[32] Y. Zhang and J. Callaway, Phys. Rev. B **39**, 9397 (1989).
[33] J. Taylor, H. Guo, and J. Wang, Phys. Rev. B **63**, 245407 (2001).
[34] S. J. Tans, M. H. Devoret, H. Dai, A. Thess, R. E. Smalley, L. J. Geerligs, and C. Dekker, Nature (London) **386,** 474 (1997) .
[35] J. J. Palacios, A. J. Pérez-Jiménez, E. Louis, E. SanFabián, and J. A. Vergés, Phys. Rev. Lett. **90**, 106801 (2003) .